Analytical Biochemistry 413 (2011) 43–49

Contents lists available at ScienceDirect

Analytical Biochemistry

journal homepage: www.elsevier.com/locate/yabio

Characterization of Förster resonance energy transfer in a botulinum neurotoxin protease assay

Justin A. Ross [a], Marcella A. Gilmore [b], Dudley Williams [b], K. Roger Aoki [b], Lance E. Steward [b], David M. Jameson [a,*]

[a] Department of Cell and Molecular Biology, John A. Burns School of Medicine, University of Hawaii, Honolulu, HI 96813, USA
[b] Department of Biological Sciences, Allergan, Irvine, CA 92612, USA

ARTICLE INFO

Article history:
Received 1 November 2010
Received in revised form 28 January 2011
Accepted 29 January 2011
Available online 3 March 2011

Keywords:
DARET
FRET
Botulinum neurotoxin
BFP
GFP
Polarization
Lifetimes

ABSTRACT

Our previous article described a fluorescence-based assay for monitoring the proteolytic activity of botulinum neurotoxin types A and E (BoNT/A and BoNT/E). As detailed in that article, the assay is based on depolarization due to Förster resonance energy transfer between blue fluorescent protein (BFP) and green fluorescent protein (GFP) moieties linked via residues 134–206 of SNAP-25 (synaptosome-associated protein of 25 kDa), the protein substrate for BoNT/A and BoNT/E. Before cleavage of this recombinant substrate, the polarization observed for the GFP emission, excited near the absorption maximum of the BFP, is very low due to depolarization following energy transfer from BFP to GFP. After substrate cleavage and diffusion of the fluorescent proteins beyond the energy transfer distance, the polarization is high due to observation of the emission only from directly excited GFP. This change in fluorescence polarization allows an assay, termed DARET (depolarization after resonance energy transfer), that is robust and sensitive. In this article, we characterize the spectroscopic parameters of the system before and after substrate cleavage, including excitation and emission spectra, polarizations, and lifetimes.

Polarized fluorescence from solutions of fluorescein and other xanthene-based fluorophores was first observed in 1920 by Weigert [1], who noted that polarization increased as the molecular rotation of the fluorophore decreased. Perrin soon developed the theoretical foundations for depolarization of fluorescence due to Brownian rotation of the fluorophore [2], and this technique was introduced into biochemistry by Weber during the 1950s and 1960s. Laurence, working with Weber's polarization instrument, first measured the binding of fluorophores to proteins using fluorescence polarization [3], and during the 1960s Dandliker and coworkers [4,5] used fluorescence polarization to follow antigen–antibody interactions, thereby initiating the field of fluorescence polarization immunoassays (FPIAs)[1]. During the late 1970s to early 1980s, Abbott Laboratories developed a commercial instrument designed to use fluorescence polarization-based immunoassays to quantify specific antigens in biological fluids. This instrument, the TDx, was extremely successful commercially and helped to popularize fluorescence polarization-based assays in the clinical chemistry field [6]. All of these fluorescence polarization approaches to ligand binding and biological assays used the fact that changes in rotational diffusion of the fluorophore give rise to the observed changes in polarization. A recent review covered historical aspects, theory, and practice of fluorescence polarization/anisotropy applied to ligand binding and assays [7].

In 1924, Gaviola and Pringsheim [8] described the concentration-dependent depolarization of fluorescein in viscous solvents (i.e., solvents that did not allow for significant rotational diffusion of the fluorophores during their excited state lifetime). This depolarization was recognized as being due to transfer of excited state energy between fluorophores in proximity and was the motivation for early treatments of resonance energy transfer that eventually led to modern theories of Förster resonance energy transfer (FRET). Theories of depolarization after such self-transfer (also termed homotransfer) were given by Weber [9] and several other researchers (reviewed in Ref. [10]). This approach has been used in protein chemistry to study processes such as protein subunit exchange [11–14] and to follow protein association inside living cells [15–17].

Depolarization due to heterotransfer (i.e., between different molecular species) was also observed years ago. Among the earliest reports of this phenomenon was Weber's observation of depolarization of tryptophan fluorescence in proteins due to FRET from

* Corresponding author.
E-mail address: djameson@hawaii.edu (D.M. Jameson).

[1] *Abbreviations used:* FPIA, fluorescence polarization immunoassay; FRET, Förster resonance energy transfer; DARET, depolarization after resonance energy transfer; BoNT, botulinum neurotoxin; GFP, green fluorescent protein; BFP, blue fluorescent protein; FLIM, fluorescence lifetime imaging microscopy; CFP, cyan fluorescent protein; YFP, yellow fluorescent protein; SNAP25, synaptosome-associated protein of 25 kDa; rLC/A, recombinant type A light chain.

0003-2697/$ - see front matter © 2011 Elsevier Inc. All rights reserved.
doi:10.1016/j.ab.2011.01.045

excited tyrosine residues [18,19]. Although most modern hetero-FRET experiments rely on changes in intensity or lifetime, as Weber's early work showed, it is also possible to use changes in polarization to monitor changes in FRET efficiency. The DARET (depolarization after resonance energy transfer) assay described in our previous article [20] uses such polarization changes to follow cleavage of a peptide substrate for botulinum neurotoxin type A (BoNT/A).

During the years following the initial report of the isolation and spectral properties of green fluorescent protein (GFP) from the *Aequorea victoria* jellyfish [21], a great many mutations were introduced into the protein backbone using site-directed mutagenesis to alter the absorption and emission properties of the chromophore (see, e.g., Ref. [22]). One of the first such mutations was the change of tyrosine at position 66 to histidine, which gave rise to a blue-shifted emission [23]. This mutant was subsequently named blue fluorescent protein (BFP) and was the first in a series of blue-shifted fluorescent proteins. The particular GFP and BFP proteins used in the current study are described in our previous article [20].

The first FRET-based assay using BFP to GFP transfer was for factor X protease [24]. The initial motivation for the development of different fluorescent proteins was to create systems with enhanced brightness and spectral properties (absorption and emission) more suitable for conventional fluorescence microscopy. Soon, however, an additional motivation was to develop donor–acceptor pairs with the highest possible Förster critical transfer distance (R_0). Nearly all of the approaches to this problem concerned improving the overlap integral between the donor emission and the acceptor absorption spectra.

Most FRET measurements with fluorescent protein systems have been done using fluorescence intensity, often using the ratio of intensities taken at two wavelengths (e.g., the emission maxima of the donor and acceptor). During recent years, the development of fluorescence lifetime imaging microscopy (FLIM) has led to the use of lifetime determinations on the donor to ascertain changes in FRET efficiency resulting from some type of perturbation (e.g., binding or release of ligands such as calcium, changes in protein–protein interactions). Nagai and coworkers [25], recognizing that FRET efficiency in a donor–acceptor pair depends on the relative orientation of the two dipoles, synthesized a variety of cyan fluorescent protein–yellow fluorescent protein (CFP–YFP) calcium sensor systems with altered orientations and noted that the anisotropy/polarization changed on calcium binding, with the largest change being 0.17 in anisotropy. This result clearly indicated that the orientation of the donor and acceptor system changed on ligand binding. Although many "new and improved" FRET fluorescent protein pairs have been described, a BFP–GFP pair can result in excellent FRET characteristics, as shown in this article. Moreover, as shown in this study, the original BFP–GFP FRET pair offers certain advantages over other popular fluorescent protein FRET pairs currently in use.

Materials and methods

Steady state fluorescence

GFP–SNAP25 (synaptosome-associated protein of 25 kDa)–BFP, GFP–SNAP25, and BFP–SNAP25 were isolated and purified as described in our previous article [20]. Absorption spectra were measured using a UV-2401PC absorption spectrophotometer (Shimadzu, Kyoto, Japan) with 5-nm slit widths. Steady state fluorescence measurements were conducted on an ISS PC1 steady state fluorimeter (ISS, Champaign, IL, USA) using a xenon lamp as the excitation source. Emission spectra were corrected for the polarization dependence of the emission monochromator and the wavelength-dependent response of the photomultiplier tube (PMT) using correction files provided by ISS traceable to an NBS (National Bureau of Standards) calibrated standard lamp. Corrected excitation spectra were obtained by correcting for the wavelength dependence of the lamp/excitation monochromator output. The lamp spectrum was determined using a 3-mm square cuvette containing 10 mM rhodamine B (Sigma, St. Louis, MO, USA) in spectroscopic-grade ethanol (Sigma) by scanning the excitation wavelength and monitoring the emission at 620 nm. The cuvette was carefully positioned such that fluorescence emission from the front face of the cuvette was optimally collected with minimal scattered light. Slit widths were 4 and 16 nm for the excitation and emission monochromators, respectively, and the excitation polarizer was vertical to eliminate polarization artifacts (e.g., Wood's anomalies) from the excitation monochromator [26].

Time-resolved fluorescence

Frequency domain time-resolved spectroscopy (see, e.g., Ref. [27]) was conducted on an ISS Chronos fluorimeter using 375- or 471-nm laser diodes for excitation. Excitation and emission polarizers were set parallel and 55°, respectively, to the vertical laboratory axis to eliminate polarization effects [28]. On exciting with the 375-nm laser diode (in conjunction with a 375/6-nm bandpass excitation filter [Semrock, Rochester, NY, USA]), dimethyl-POPOP (1,4-bis-(5-phenyloxazolyl-2-)-benzene) in ethanol was used as the fluorescence lifetime reference (1.45 ns). On excitation with the 471-nm laser diode (with 482/18-nm bandpass excitation filter [Semrock]), fluorescein (Sigma) in 0.01 M NaOH was used as the lifetime reference (4.05 ns). Modulation frequencies were chosen such that the phase delay stayed within the range of 15–75°. GFP emission at wavelengths greater than 525 nm was isolated using a Corning longpass filter (product no. 3484), whereas the BFP emission was isolated using a 435/40-nm bandpass filter (Semrock). All fluorescence measurements were made in 10 × 4-mm Spectrosil quartz cuvettes (Starna Cells, Atascadero, CA, USA). Frequency domain data were analyzed using Globals for Spectroscopy (Laboratory for Fluorescence Dynamics, University of California, Irvine).

Quantum yield determination

The fluorescence quantum yield of the BFP was determined relative to quinine sulfate in 0.1 M sulfuric acid at 22 °C by exactly matching the optical density at the excitation wavelength (368 nm) of the sample and reference. The published quantum yield of quinine sulfate under similar conditions varies from 0.48 [29] to 0.70 [30]; for this treatise, the value of 0.546 [31] was used. The total emission was collected using a 400-nm longpass filter (KV 399, Schott, San Jose, CA, USA). The spectral bandwidths of the absorption spectrometer and excitation monochomator were matched as closely as possible (5 and 4 nm, respectively). The extinction coefficients of BFP and GFP were determined using the bicinchoninic acid (BCA) assay method as described in Ref. [32].

Results and discussion

The absorption spectra of BFP–SNAP25, GFP–SNAP25, and the GFP–SNAP25–BFP substrate are shown in Fig. 1A. Although the maximum near 385 nm is due primarily to BFP, there is some absorption in this region due to GFP. Within the GFP–SNAP25–BFP substrate, the absorption at 375 nm (the wavelength used in the time-resolved and polarization measurements) due to the GFP is approximately 8%. The absorption peak near 490 nm is, however, due entirely to GFP. Also of note is the slight red shift of the absorption of GFP within the GFP–SNAP25–BFP substrate compared with GFP–SNAP25. The corrected emission spectra of

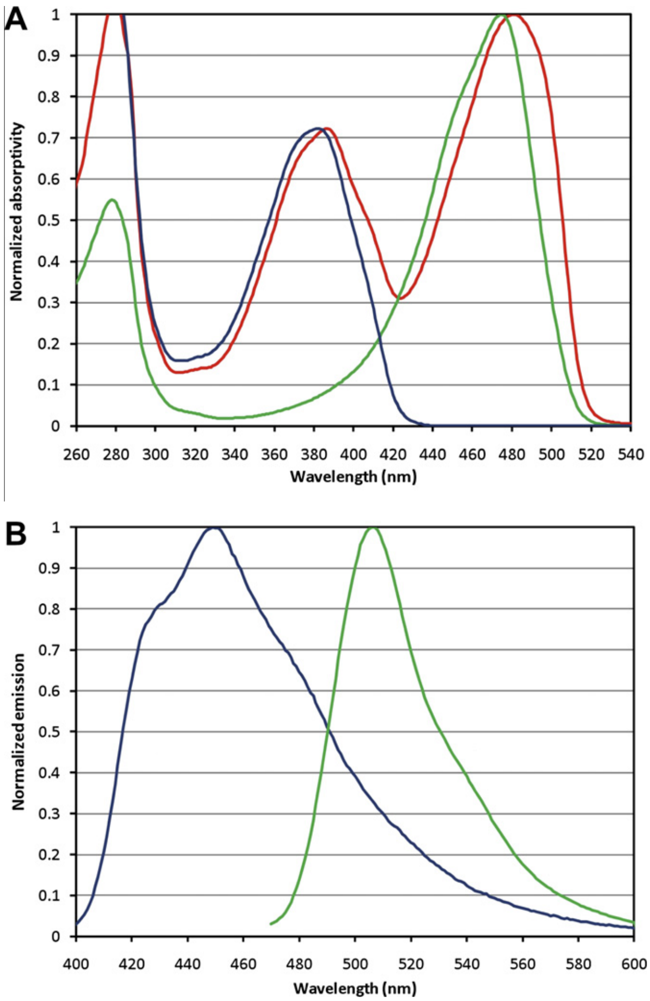

Fig.1. (A) Absorption spectra of GFP–SNAP25 (green), BFP–SNAP25 (blue), and GFP–SNAP25–BFP (red). (B) Normalized corrected emission spectra of BFP–SNAP25 (blue) and GFP–SNAP25 (green). Excitation was at 375 nm (BFP) and 460nm (GFP).

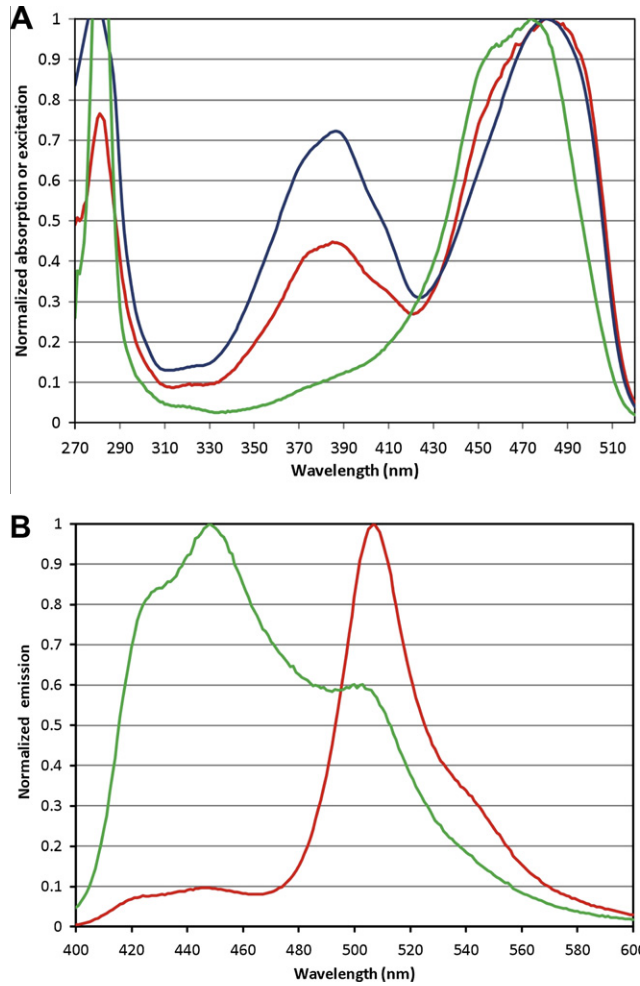

Fig.2. (A) Corrected excitation spectra of the intact (red) and cleaved (green) substrate. Emission was observed at 560 nm. For comparison, the absorption spectrum of GFP–SNAP25–BFP (blue) is also shown. (B) Corrected emission spectra for intact (red) and cleaved (green) GFP–SNAP25–BFP. Excitation was at 375 nm.

BFP–SNAP25 and GFP–SNAP25 are shown in Fig. 1B. The corrected excitation spectra of BFP–SNAP25, GFP–SNAP25, and GFP–SNAP25-BFP are shown in Fig. 2. The slight red shift of the GFP peak in the GFP–SNAP25–BFP substrate seen in the absorption spectrum is also present in the excitation spectra. Typically, a change in the absorption spectrum of a compound is associated with a change in ground state interactions, and this observed change may be indicative of direct interaction of the BFP and GFP moieties (discussed below). A substantial increase in intensity is seen in the BFP peak for the intact GFP–SNAP25–BFP substrate compared with the cleaved BFP due to the FRET from the BFP to the GFP.

The emission peaks of BFP and GFP are at 448 and 505 nm, respectively (Fig. 1B). Consistent with the change of the excitation spectrum, the emission spectrum of GFP–SNAP25–BFP, when excited at 375 nm, also changes when cleaved, with the GFP emission being substantially reduced while the BFP emission increases (Fig. 2B).

Excitation polarization spectra for GFP emission in the intact and cleaved GFP–SNAP25–BFP are shown in Fig. 3A. The difference in polarization between the intact and cleaved substrate demonstrates that the optimal wavelength range to achieve the greatest change in polarization on substrate cleavage, approximately 0.4, occurs between 350 and 375 nm. The optimal excitation wavelength for the assay, regarding intensity and polarization change, is approximately 375 nm. This wavelength provides near maximal change in the polarization when the substrate is cleaved and near maximal absorption due to the BFP. At excitation wavelengths longer than 425 nm, the change of the polarization is negative at approximately −0.025 (Fig. 3A). The change of the polarization above 425 nm excitation is not associated with depolarization due to energy transfer; rather, it is caused by the increase in the rotational relaxation time of the fluorophore due to the reduced size of the rotating moiety (i.e., GFP–SNAP25 vs. GFP–SNAP25–BFP). The emission polarization scans of the cleaved and intact substrate (Fig. 3B) illustrate the importance of choosing an appropriate emission wavelength or filter. Emission wavelengths less than 470 nm result in a minimal change on proteolysis; hence, for maximal change of the polarization, emission greater than 510 nm should be collected. The data in Fig. 3A were collected using a 537-nm longpass filter (Corning, product no. 3484) that almost completely eliminates emission from the BFP, which would reduce the polarization change.

Some fluorescent proteins, such as the ones used in this assay, have been reported to form dimers at high concentrations [33,34]. The presence of BFP–GFP or GFP–GFP dimers, after cleavage of the substrate, actually explains some observations. Namely, we observed that the final polarization reached after substrate cleavage was dependent on the concentration of the substrate (Fig. 4). As shown in Fig. 4, there appears to be both BFP–GFP and GFP–GFP dimers present, and we assume that BFP–BFP dimers could also

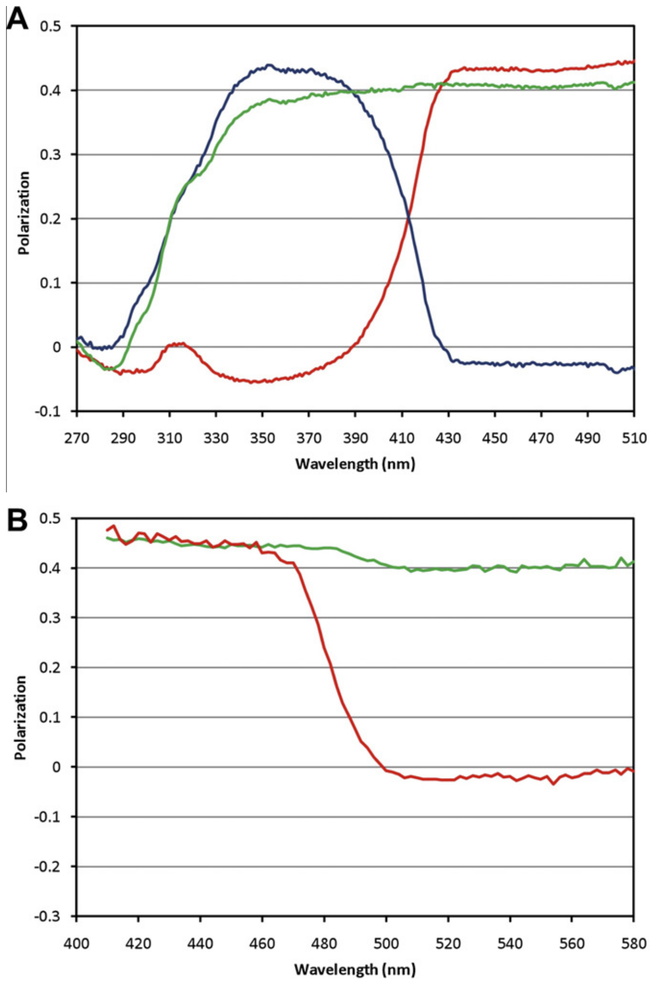

Fig.3. (A) Excitation polarization spectrum of intact (red) and cleaved substrate with rLC/A (green) GFP–SNAP25–BFP. Emission was observed through a 527-nm longpass filter in both cases. The change in the polarization on cleavage is represented by the blue curve. (B) Emission polarization scan of intact (red) and cleaved (green) GFP–SNAP25–BFP exciting at 375 nm.

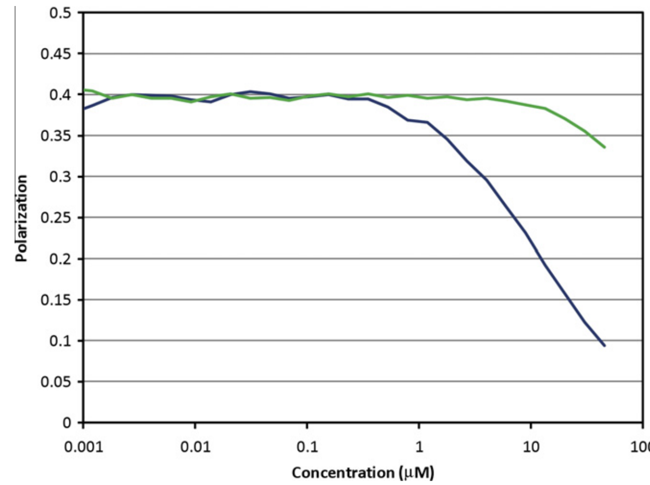

Fig.4. Serial dilution of GFP–SNAP25–BFP cleaved with trypsin exciting at 375 nm (blue) and 480 nm (green) collecting emission through a 537-nm longpass filter.

Table 1
Results of the data analysis.

Sample	τ_1 (ns)	τ_2 (ns)	$\chi2$	ρ (ns)	χ^2
Intact GFP–SNAP25–BFP (Ex 375, Em BFP)	1.57 (71%)	0.55 (29%)	1.69		
GFP–SNAP25–BFP (Ex 471, Em GFP)	3.07 (100%)		0.78	91.9 (0.39)	0.08
Cleaved GFP–SNAP25–BFP (Ex 375, Em BFP)	1.49 (91%)	0.4 (9%)	1.60		
Cleaved GFP–SNAP25–BFP (Ex 471, Em GFP)	3.09 (100%)		2.01	52.9 (0.39)	0.08

Note: Chi-square ($\chi2$) values were calculated as indicated in Ref. [27]. For lifetime analysis, standard errors for phase and modulation of 0.2 and 0.004, respectively, were used. The last three columns show the rotational relaxation times and associated anisotropies and the chi-square values associated with the fits.

exist. It is difficult to accurately determine the K_d for the dimerization processes from Fig. 4, but it appears to be consistent with a K_d in the range of 100–200 μM, which agrees with previously reported values based on analytical ultracentrifugation [35]. The interaction of the cleaved BFP and GFP is also seen at higher concentrations, but at 3 M GuHCl an increase in the polarization to the level reached at sub-100-nM concentrations was obtained (data not shown). At concentrations of cleaved substrate less than 500 nM, the polarization of the cleaved fraction is 0.39, whereas at higher concentrations, the polarization decreases due to energy transfer between the complexed BFP and GFP fragments. When using the DARET assay to investigate kinetics of a proteolytic process, one would typically be interested only in the initial region of the assay where the cleaved substrate fraction is very small compared with the total substrate concentration; thus, at no stage will there be a concentration of associated cleaved fluorescent proteins to appreciably affect the measurement.

Time-resolved data on these systems are shown in Fig. S1 in the supplementary material, with Table 1 listing the results of the data analysis. The lifetime of the GFP remains essentially unchanged in the intact or cleaved substrate at approximately 3.1 ns (although in the intact substrate there is a slight phase delay as expected in the phase data due to the energy transfer [data not shown]). The BFP lifetime is reduced in the intact substrate due to the energy transfer from 1.57 ns (71%) and 0.55 ns (29%) to 1.49 ns (91%) and 0.4 ns (9%), respectively.

The rotational relaxation times of the intact substrate, observed via either the BFP or GFP emissions, are consistent with a single rotator with no local motion of the chromophore (Fig. 5) [26]. This conclusion is supported by the decrease in the phase delay at high frequencies and suggests that the conformation of the substrate is such that the BFP and GFP moieties are not freely rotating with respect to one another but rather rotate together as a single unit. The rotational relaxation time of the BFP–SNAP25 cleavage product is similar to that of free GFP, whereas the GFP–SNAP25 cleavage pro is larger, consistent with the cleavage site being closer to the BFP.

As shown in Fig. 3 as well as in our previous article [20], excitation of the intact GFP–SNAP25–BFP near the BFP absorption maximum and observation of the emission of GFP lead to a very low polarization value. Cleavage of the GFP–SNAP25–BFP peptide by BoNT/A, recombinant type A light chain (rLC/A), or trypsin, however, results in a high polarization for the GFP emission. This original low polarization is due to FRET from the excited BFP to the GFP. Specifically, the orientation of the BFP transition dipole is at a relatively large angle with respect to the GFP absorption dipole, as depicted in Fig. 6. As detailed in Appendix A, this value was calculated to be 70°.

To investigate the stability of the GFP–SNAP25–BFP and the relative BFP–GFP orientation and distance, the polarization of GFP–SNAP25–BFP, on 385 nm excitation with emission observed using a 537-nm longpass filter (Corning, product no. 3484), was measured as a function of GuHCl concentration (Fig. 7). One observes that the polarization decreases slightly at 100 mM GuHCl, with this

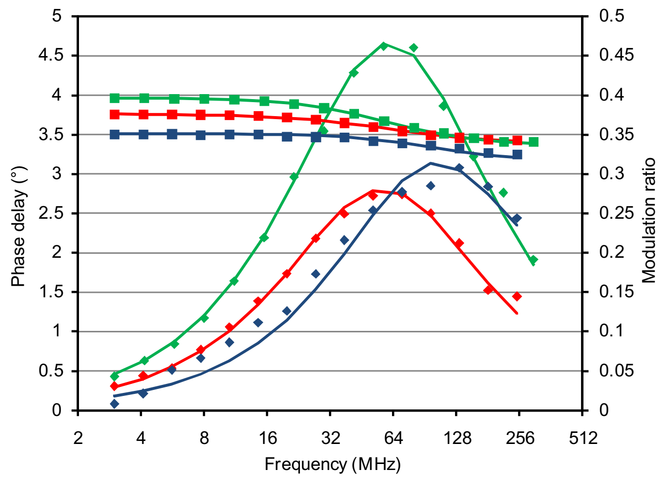

Fig.5. Dynamic polarization data of intact GFP–SNAP25–BFP monitoring GFP (red) and cleaved GFP–SNAP25–BFP exciting and detecting the BFP (blue) and GFP (green). Symbols represent data points, and lines represent fits to the data.

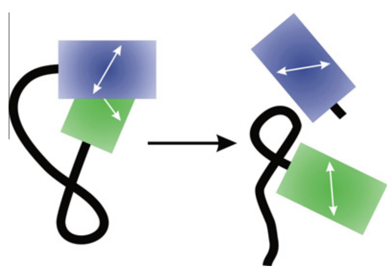

Fig.6. Depiction of GFP–SNAP25–BFP before and after cleavage. Note that it is the acute angle between the dipoles that is used in the determination of κ^2.

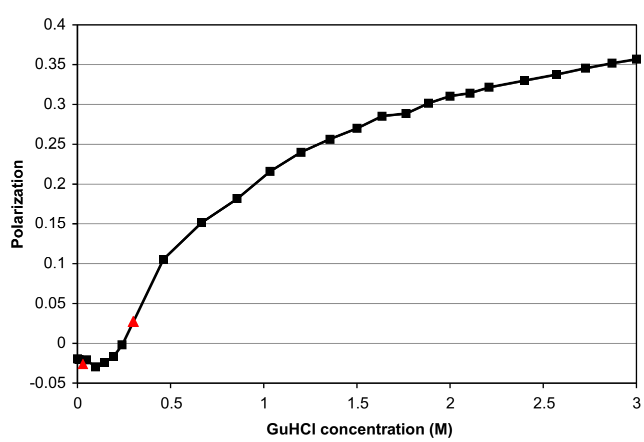

Fig.7. Effect of GFP–SNAP25–BFP polarization with increasing GuHCl (black squares; solid line is a guide for the eye). GFP–SNAP25–BFP in 3 M GuHCl diluted 10-fold and 100-fold (red triangles).

decrease indicating a slight increase in the energy transfer efficiency. As the GuHCl concentration increases, the polarization increases due to the reduced energy transfer as the fluorescent protein moieties separate. Due to the resilient β-barrel structure of the fluorescent proteins, even 3 M GuHCl does not result in their denaturation [36]; however, the SNAP25 domain will unfold. The substrate was not irreversibly denatured, as illustrated by the return of the polarization values to their initial values on dilution into GuHCl free buffer (see red triangles in Fig. 7 at approximately 0.03 and 0.3 M GuHCl).

The Förster critical radius (R_0) over which the energy transfer efficiency falls to 50% is given by

$$R_0 = 0.2108\left[\kappa^2 \phi_D n^{-4} \int_0^{\infty} I_D(\lambda)\varepsilon_A(\lambda)\lambda^4 d\lambda\right]^{1/16}, \tag{1}$$

where κ^2 is the orientation factor, I_D is the quantum yield of the BFP donor (0.21), n is the refractive index of the medium (1.4) [37], and $I_D(\lambda)$ and $\varepsilon_A(\lambda)$ are the normalized donor fluorescence emission spectrum and acceptor extinction coefficient spectrum as a function of wavelength (λ), respectively. The extinction coefficients of the GFP and BFP used in this treatise have not been reported previously, but they were determined by us to be 50,400 ± 800 M^{-1} cm^{-1} (475 nm) and 28,000 ± 1000 M^{-1} cm^{-1} (375 nm), respectively. From this equation, one can calculate a value of R_0 that is independent of the κ^2 value, termed $R_0' = R_0/(\kappa^2)^{1/6}$ = 37 Å. The upper and lower limits of κ^2 can be determined from the limiting polarization values of the donor and acceptor and the angle between the donor emission and acceptor absorption dipoles [10,38]. The limiting polarization values of BFP and GFP were determined to be 0.480 and 0.475, respectively. The angle between the donor and acceptor was calculated to be 70° (Appendix A). From these values, the maximum and minimum values of κ^2 as determined from the Dale–Eisinger–Blumberg plots [38] were found to be 2.6 and 0.05, respectively. Thus, the range of R_0 values is from 43 Å (κ^2 = 2.6) to 22 Å (κ^2 = 0.05).

FRET efficiency

The efficiency of the FRET process can be estimated from both the fluorescence intensity and lifetime data. Based on the increase of the excitation spectrum, the calculated energy transfer efficiency is 34% calculated from Eq. (2) [39]:

$$A = \varepsilon_A + E\varepsilon_D, \tag{2}$$

where A is the magnitude of the excitation spectrum of the energy acceptor, E is the energy transfer efficiency, and ε_D and ε_A are the extinction coefficients of the donor and acceptor, respectively. From the integrated change in the corrected emission spectra of the GFP emission, before and after substrate cleavage (Eq. 3) [40], a FRET efficiency of 36% is calculated:

$$E = \frac{\varepsilon_A(\lambda_D)}{\varepsilon_D(\lambda_D)}\left[\frac{I_A}{I_A^0} - 1\right], \tag{3}$$

where I_A and I_A^0 are the total intensity of the acceptor in the presence and absence of the donor, respectively, at the donor excitation wavelength (λ_D).

The FRET efficiency was also determined from the fluorescence lifetime of the donor from Eq. (4) [37]:

$$E = 1 - \frac{\tau_D}{\tau_D^0}, \tag{4}$$

where τ_D and τ_D^0 are the fluorescence lifetime of the donor in the presence and absence of the acceptor, respectively. Due to the multiexponential decay of the BFP in the presence and absence of the acceptor, τ_D and τ_D^0 must be calculated from the amplitude averaged lifetime $\langle\tau\rangle$ values (Eq. 5) [41]:

$$\langle\tau\rangle = \frac{\sum_i \alpha_i \tau_i}{\sum_i \alpha_i}, \tag{5}$$

where α_i and τ_i are the preexponential amplitude and lifetime value of the ith lifetime component, respectively. The lifetime components of the substrate cleaved and intact are given in Table 1. The average lifetime of the BFP increased from 1.02 to 1.17 ns following proteolysis, resulting in an energy transfer efficiency of 13%.

Accurately quantifying the energy transfer efficiency in a fluorescent protein FRET system can be problematic for several reasons. First, less than 100% of the chromophores within fluorescent proteins develop, leaving a fraction of the proteins "dark". In the case where the BFP chromophore has not developed, only emission from the directly excited GFP will be seen, hence not affecting the BFP intensity or lifetime. However, if the GFP chromophore does not mature, then this BFP will have its native fluorescence lifetime and intensity regardless of proteolysis of the SNAP25 domain. The lifetime of the fraction of molecules without GFP cannot be resolved from the lifetime of the quenched BFP. The presence of the longer lifetime BFP population serves to increase the measured lifetime, leading to an overestimate of the lifetime in the presence of energy transfer. Alternatively, if the donor undergoes a very high efficiency of energy transfer, then its lifetime will be very short and its fluorescence quantum yield will be greatly reduced. This situation results in the fraction of molecules without acceptors (which still possess the higher quantum yield) contributing the majority of the emission to the measurement. These factors, combined with the multiexponential decay behavior of the BFP, contributed to the lower estimate of the energy transfer when calculated from the time-resolved measurements.

Both GFP and BFP are barrel-shaped proteins composed of 11 antiparallel β-sheets [34] with some α-helical stretches. The chromophore in both cases is due to the oxidation and rearrangement of three amino acids, namely at positions 65, 66, and 67. The chromophore is situated near the center of the protein, and its absorption dipole is oriented at approximately 60° with respect to the long axis of the protein barrel [42]. Based on the energy transfer efficiencies and the range of κ^2 values, the possible range of distances between the BFP and GFP can be calculated. From the excitation spectrum, the range is 25–48 Å; from the emission spectrum, the range is 25–48 Å; and from the time-resolved data, the range is 31–59 Å. The dimensions of the β-barrel of the fluorescent proteins are approximately 30 Å across and 42 Å long. Thus, for the lower range of distances, the β-barrels of the BFP and GFP would be in contact. The slight shift of the absorption spectrum of the GFP and the observed interaction of the cleaved BFP and GFP (Fig. 5) combined with the single rotational relaxation time (which is consistent with the size of the intact substrate as opposed to the rotational rate that one might expect from a GFP moiety free to rotate independently) suggest that they are most likely in contact in the intact substrate. The fluorescent proteins used in this assay have not had the numerous mutations to remove the sites of interaction that other variants have had. However, the presence of this interaction allows significant energy transfer and a large polarization change using the original BFP and GFP moieties. Other BoNT/A substrates based on SNAP25 and using FRET between fluorescent proteins have been developed, but the changes detected on proteolysis are much less (e.g., Ref. [43]). We postulate that even though the spectral overlap between the CFP and YFP used in Dong and coworkers' assay was larger, the absence of any direct interaction resulted in the proteins not being in contact despite their being tethered, resulting in a larger mean separation and, hence, less efficient energy transfer [43].

The large change in the polarization on cleavage of the substrate is due primarily to the large angle between the absorption dipole of the acceptor and the emission dipole of the donor combined with the detection of only the emission from the acceptor. The change of angle is manifested through a change in the effective P_0 in the Perrin equation due to the energy transfer. Although there is also a change in the rotational volume, this effect, given the relatively short fluorescence lifetime, contributes much less to the change in the polarization than does the effect of the angle. The excitation and emission wavelengths of the experiment were chosen specifically to result in the most pronounced change in polarization.

We note that a value of 2/3 is almost always adopted for κ^2 based on the assumption of "dynamic averaging" between the dipoles. However, dynamic averaging should apply only when the dipoles can move appreciably during the excited state lifetimes of the donor and acceptor (when the acceptor is fluorescent). In the case of fluorescent proteins (e.g., BFP, GFP) that have relatively short fluorescence lifetimes compared with their rotational rates, especially when they are attached to other moieties, the dynamic averaging assumption cannot be rigorously justified.

Conclusions

Our previous article [20] demonstrated the usefulness of the DARET assay, in both regular and high-throughput formats, to monitor the proteolytic activity of BoNT/A and to determine kinetic constants. In this article, we have examined the photophysics underlying this assay. Although many FRET-based assays and FRET-based biosensors have been described, to our knowledge the DARET assay is the first such polarization-based FRET assay. One intrinsic advantage of this type of assay is that the polarization (or anisotropy) values are intrinsic parameters that are platform independent. When coupled with protease measurements, a DARET assay also has the advantage that the measured parameters can be directly related to the number of product molecules formed, facilitating determination of kinetic parameters, as illustrated in our previous article [20].

Acknowledgment

We thank Nicholas James for assistance in the determination of the extinction coefficients of BFP and GFP and for helpful discussions.

Appendix A. Calculation of the angle between BFP and GFP

Note. For convenience of illustration, anisotropy is used throughout Appendix A, whereas polarization is used throughout the body of the article.

In the intact substrate, the following species can contribute to the anisotropy:

1. Directly excited BFP
2. Directly excited GFP; and
3. GFP excited via FRET from BFP.

Both species 1 and 2 are also present whether the substrate is cleaved or intact, whereas specie 3 is present only for the intact substrate.

Let $f_{BBi} + f_{GGi} + f_{BGi} = 1$, where f indicates the fraction of the total GFP emission and where the subscripts BB, GG, and BG denote species with excitation and emission from BFP, excitation and emission from GFP, and excitation of BFP followed by FRET to GFP, respectively, and the subscripts i and c denote intact and cleaved substrate, respectively.

From the Perrin equation and the data in Table 1, $r_0/r = 1 + 3\tau/\rho$; therefore, using the values determined in the article, $r_{GGi} = 0.333$.

Assuming that the only factor responsible for the change of fluorescence intensity measured is due to the reduction in the amount of energy transfer, the intensity of the 100% cleaved substrate will be due solely to that from the directly excited GFP specie. In addition, the fractional intensities will be proportional to the species fractions, that is, $I_{GGc}/I_{BGc} = f_{GGc}/f_{BGc}$, $I_i = I_{GGi} + I_{BGi} = 950 \times 10^3$ cps, and $I_f = I_{GGc} = 186 \times 10^3$ cps. Therefore, $f_{BGi} = 0.84$ and $f_{GGi} = 0.16$.

Thus, the anisotropy of the intact substrate undergoing energy transfer $r_{BGi} = -0.088$.

Taking into account each of the depolarizing processes within the intact substrate exhibiting energy transfer – that is, depolarization due to the angle between the absorption and emission dipoles of BFP (11.8°), the emission dipole of BFP and the absorption dipole of GFP (θ), the absorption and emission dipoles of GFP (11.2°, r_0 GFP = 0.377 [430 nm]), and finally the rotational molecular motion (16.7°) that has occurred during the excited state lifetime, we can calculate θ using the Soleillet theorem [44,45]:

$$r = \frac{2}{5}\pi_i d_i,$$

where $d_i = (3/2\cos^2\theta_i - ½)$ and θ_i is the depolarization through angle θ_i for the ith depolarizing process. From this equation, the angle between the emission dipole of the BFP and the absorption dipole of the GFP is 70°.

Appendix B. Supplementary data

Supplementary data associated with this article can be found, in the online version, at doi:10.1016/j.ab.2011.01.045.

References

[1] F. Weigert, Uber polarisiertes Fluoreszenzlicht, Verh. Dtsch. Phys. Ges. 1 (1920) 100–102.
[2] F. Perrin, Polarisation de la Lumiere de Fluorescence: Vie Moyene des Molecules Fluorescentes, J. Physique 7 (1926) 390–401.
[3] D.J.R. Laurence, A study of the adsorption of dyes on bovine serum albumin by the method of polarization of fluorescence, Biochem. J. 51 (1952) 168–180.
[4] W.B. Dandliker, G.A. Feigen, Quantification of the antigen–antibody reaction by the polarization of fluorescence, Biochem. Biophys. Res. Commun. 5 (1961) 299–304.
[5] W.B. Dandliker, S.P. Halbert, M.C. Florin, R. Alonso, H.C. Schapiro, Study of penicillin antibodies by fluorescence polarization and immunodiffusion, J. Exp. Med. 122 (1965) 1029–1048.
[6] M.E. Jolley, S.D. Stroupe, C.H. Wang, H.N. Panas, C.L. Keegan, R.L. Schmidt, K.S. Schwenzer, Fluorescence polarization immunoassay: I. Monitoring aminoglycoside antibiotics in serum plasma, Clin. Chem. 27 (1981) 1190–1197.
[7] D.M. Jameson, J.A. Ross, Fluorescence polarization/anisotropy in diagnostics and imaging, Chem. Rev. 110 (2010) 2685–2708.
[8] E. Gaviola, P. Pringsheim, Uber den Einfluss der Konzentration auf die Polarisation der Fluoreszenz von Farbstofflosenungen, Z. Physik 24 (1924) 24–36.
[9] G. Weber, Dependence of the polarization of the fluorescence on the concentration, Trans. Faraday Soc. 50 (1954) 552–556.
[10] B.W Van Der Meer, G. Coker, S. Y. S Chen, Resonance Energy Transfer: Theory and Data, Wiley-VCH, New York, 1991.
[11] L. Erijman, G.H. Lorimer, G. Weber, Reversible dissociation and conformational stability of dimeric ribulose bisphosphate carboxylase, Biochemistry 32 (1993) 5187–5195.
[12] L. Erijman, G. Weber, Oligomeric protein associations: transition from stochastic to deterministic equilibrium, Biochemistry 30 (1991) 1595–1599.
[13] K. Ruan, G. Weber, Physical heterogeneity of muscle glycogen phosphorylase revealed by hydrostatic pressure dissociation, Biochemistry 32 (1993) 6295–6301.
[14] B.D. Hamman, A.V. Oleinikov, G.G. Jokhadze, R.R. Traut, D.M. Jameson, Dimer/monomer equilibrium and domain separations of *Escherichia coli* ribosomal protein L7/L12, Biochemistry 35 (1996) 16680–16686.
[15] I. Gautier, M. Tramier, C. Durieux, J. Coppey, R.B. Pansu, J.C. Nicolas, K. Kemnitz, M. Coppey-Moisan, Homo-FRET microscopy in living cells to measure monomer–dimer transition of GFP-tagged proteins, Biophys. J. 80 (2001) 3000–3008.
[16] M. Tramier, M. Coppey-Moisan, Fluorescence anisotropy imaging microscopy for homo-FRET in living cells, Methods Cell Biol. 85 (2008) 395–414.
[17] M. Tramier, T. Piolot, I. Gautier, V. Mignotte, J. Coppey, K. Kemnitz, C. Durieux, M. Coppey-Moisan, Homo-FRET versus hetero-FRET to probe homodimers in living cells, Methods Enzymol. 360 (2003) 580–597.
[18] G. Weber, Fluorescence polarization spectrum and electronic-energy transfer in proteins, Biochem. J. 75 (1960) 345–352.
[19] G. Weber, Fluorescence polarization spectrum electronic energy transfer in tyrosine tryptophan and related compounds, Biochem. J. 75 (1960) 335–345.
[20] M. A. Gilmore, D. Williams, Y. Okawa, B. Holguin, N. G. James, J. A. Ross, K. R. Aoki, D. M. Jameson, L. E. Steward, Depolarization after resonance energy transfer (DARET): a sensitive fluorescence-based assay for botulinum neurotoxin protease activity, Anal. Biochem. (2011), doi:10.1016/j.ab.2011.01.043.
[21] O. Shimomura, F.H. Johnson, Y. Saiga, Extraction, purification, and properties of aequorin, a bioluminescent protein from the luminous hydromedusan, Aequorea, J. Cell. Comp. Physiol. 59 (1962) 223–239.
[22] N.C. Shaner, G.H. Patterson, M.W. Davidson, Advances in fluorescent protein technology, J. Cell Sci. 120 (2007) 4247–4260.
[23] R. Heim, D.C. Prasher, R.Y. Tsien, Wavelength mutations and posttranslational autoxidation of green fluorescent protein, Proc. Natl. Acad. Sci. USA 91 (1994) 12501–12504.
[24] R.D. Mitra, C.M. Silva, D.C. Youvan, Fluorescence resonance energy transfer between blue-emitting and red-shifted excitation derivatives of the green fluorescent protein, Gene 173 (1996) 13–17.
[25] T. Nagai, A. Sawano, E.S. Park, A. Miyawaki, Circularly permuted green fluorescent proteins engineered to sense Ca^{2+}, Proc. Natl. Acad. Sci. USA 98 (2001) 3197–3202.
[26] D.M. Jameson, J.C. Croney, Fluorescence polarization: Past present and future, Comb. Chem. High Throughput Screen 6 (2003) 167–176.
[27] J.A. Ross, D.M. Jameson, Time-resolved methods in biophysics: 8. Frequency domain fluorometry: applications to intrinsic protein fluorescence, Photochem. Photobiol. Sci. 7 (2008) 1301–1312.
[28] R.D. Spencer, G. Weber, Influence of Brownian rotations and energy transfer upon the measurements of fluorescence lifetimes, J. Chem. Phys. 52 (1970) 1654–1663.
[29] G. Zhang, Z. Li, J. Yan, Determination of the absolute fluorescence quantum yields of laser dyes using photoacoustic spectroscopy, Chin. Phys. Lett. 3 (1986) 9–12.
[30] T.G. Scott, R.D. Spencer, N.J. Leonard, G. Weber, Emission properties of NADH: Studies of fluorescence lifetime quantum efficiencies of NADH AcPyADH and simplified synthetic models, J. Am. Chem. Soc. 92 (1970) 687–695.
[31] W.H. Melhuish, Quantum efficiencies of fluorescence of organic substances: Effect of solvent and concentration of the fluorescent solute, J. Phys. Chem. 65 (1961) 229–235.
[32] G.H. Patterson, S.M. Knobel, W.D. Sharif, S.R. Kain, D.W. Piston, Use of the green fluorescent protein and its mutants in quantitative fluorescence microscopy, Biophys. J. 73 (1997) 2782–2790.
[33] R.Y. Tsien, The green fluorescent protein, Annu. Rev. Biochem. 67 (1998) 509–544.
[34] G.N. Phillips Jr., Structure and dynamics of green fluorescent protein, Curr. Opin. Struct. Biol. 7 (1997) 821–827.
[35] M. Cutler, Characterization and energy transfer mechanism of the green-fluorescent protein from *Aequorea victoria,* PhD thesis, Rutgers University, 1995.
[36] H. Fukuda, M. Arai, K. Kuwajima, Folding of green fluorescent protein and the cycle3 mutant, Biochemistry 39 (2000) 12025–12032.
[37] B. Valeur, J-C. Brochon, New Trends in Fluorescence Spectroscopy: Applications to Chemical and Life Sciences, Springer, Berlin, 2001.
[38] R.E. Dale, J. Eisinger, W.E. Blumberg, The orientational freedom of molecular probes: the orientation factor in intramolecular energy transfer, Biophys. J. 26 (1979) 161–193.
[39] L. Stryer, R.P. Haugland, Energy transfer: a spectroscopic ruler, Proc. Natl. Acad. Sci. USA 58 (1967) 719–726.
[40] B. Valeur, Molecular Fluorescence: Principles and Applications, Wiley–VCH, Weinheim, Germany, 2006.
[41] A. Sillen, Y. Engelborghs, The correct use of "average" fluorescence parameters, Photochem. Photobiol. 67 (1998) 475–486.
[42] S. Inoue, O. Shimomura, M. Goda, M. Shribak, P.T. Tran, Fluorescence polarization of green fluorescence protein, Proc. Natl. Acad. Sci. USA 99 (2002) 4272–4277.
[43] M. Dong, W.H. Tepp, E.A. Johnson, E.R. Chapman, Using fluorescent sensors to detect botulinum neurotoxin activity in vitro and in living cells, Proc. Natl. Acad. Sci. USA 101 (2004) 14701–14706.
[44] D.M Hercules, Fluorescence and Phosphorescence Analysis: Principles and Applications, Interscience, New York, 1966.
[45] P. Soleillet, Caracteres de polarisation des lumieres de fluorescence, Ann. de Phys. 12 (1929) 23.